AeroMix: a Python package for modeling aerosol optical properties and mixing state

Sam P. Raj [1], Puna Ram Sinha [1], Rohit Srivastava [2], Srinivas Bikkina [3], D. Bala Subrahamanyam [4]

[1]Department of Earth and Space Sciences, Indian Institute of Space Science and Technology Thiruvananthapuram, Kerala, 695547, India
[2] National Centre for Polar and Ocean Research, Ministry of Earth Sciences, Govt. of India, Vasco-da-Gama, Goa, 403804, India
[3] Birbal Sahni Institute of Palaeosciences, 53, University Road, Lucknow, 226007, India
[4] Space Physics Laboratory, Vikram Sarabhai Space Centre, Thiruvananthapuram, Kerala, 695022, India

Correspondence to: P. R. Sinha, (prs@iist.ac.in)

Supplementary information

S1. Evaluation of AeroMix

The consistency of AeroMix is assessed by comparing the aerosol optical and physical properties modeled with AeroMix and OPAC (Hess et al., 1998). The component-wise mass concentration compared for ten externally mixed aerosol types given in OPAC, namely continental clean, continental average, continental polluted, urban, desert, maritime clean, maritime polluted, maritime tropical, Arctic, and Antarctic at a relative humidity (RH) of 50% is presented in Fig. S1. The AeroMix computed mass concentrations of all components are consistent with the OPAC (r=0.99, slope=1; not shown).

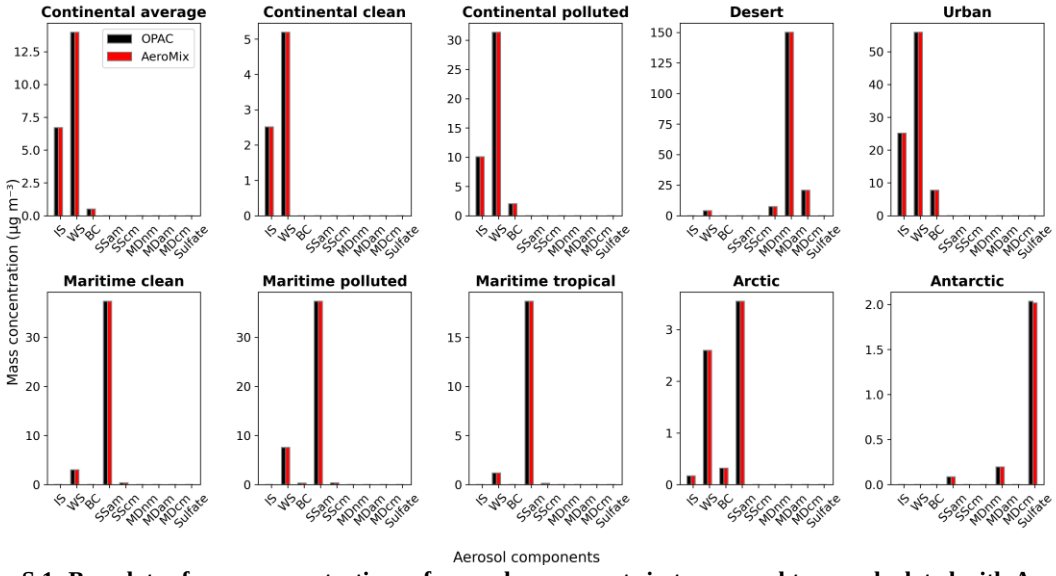

Figure S 1: Bar plots of mass concentrations of aerosol components in ten aerosol types calculated with AeroMix and OPAC at 50% relative humidity.

Similarly, the comparisons between AeroMix and OPAC modeled aerosol optical depth (AOD), single scattering albedo (SSA), and asymmetry parameter (*g*) for all wavelengths ranging from 0.25 to 40 μm are presented in Figs. S2 a-c. The optical properties such as AOD, SSA, and *g* also agree (*r*=1, slope=1) with the OPAC model (Figs. S2 a-c). Since the AOD and SSA are calculated from the modeled Mie coefficients, they need not be shown separately.

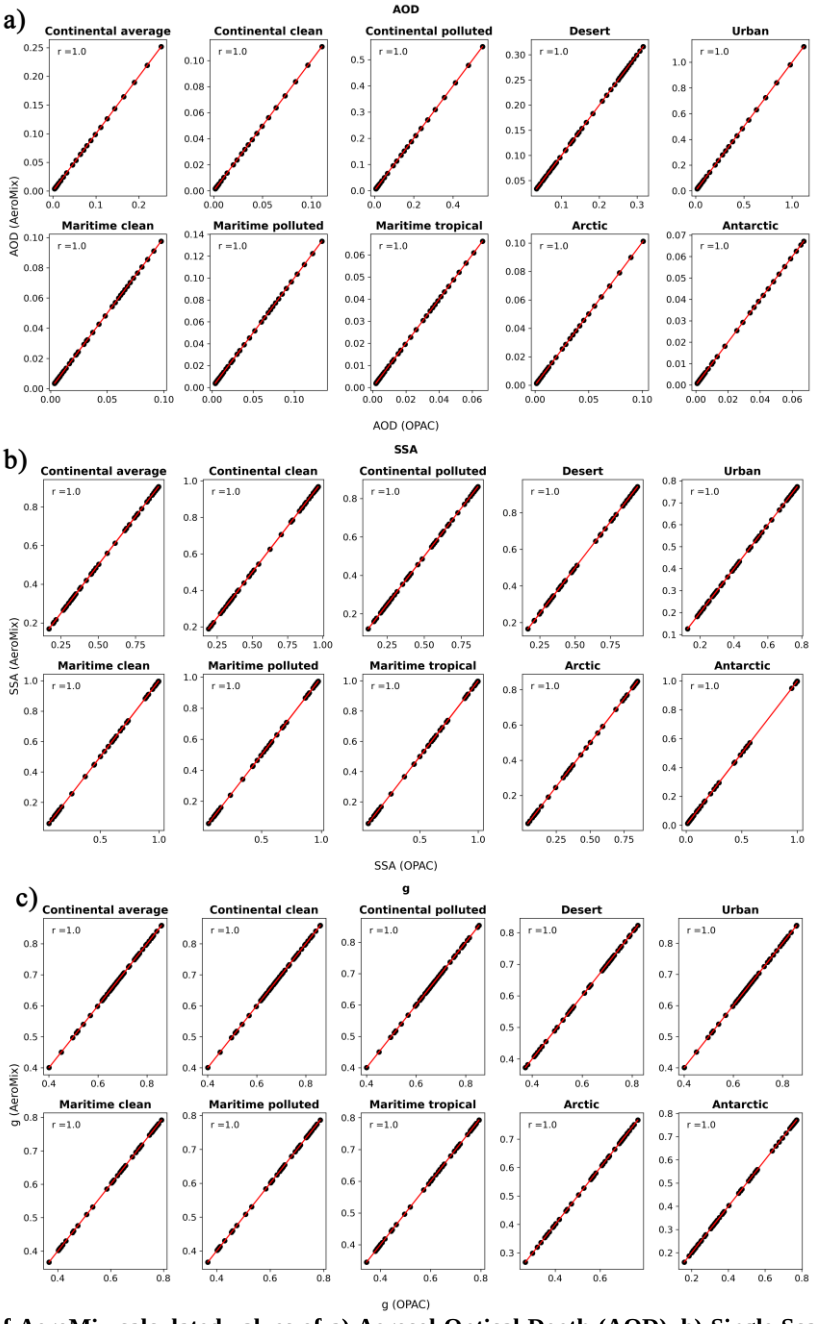

Figure S 2: Scatter plots of AeroMix calculated values of a) Aerosol Optical Depth (AOD), b) Single Scattering Albedo (SSA) and c) Asymmetry parameter (g) for ten aerosol types at relative humidity 50% for all wavelengths with those calculated by OPAC. The solid red line is the least-squares regression line forced through the origin (intercept = 0).

S2. Study region and data

S2.1 Kanpur

Kanpur (26.513° N, 80.232° E, 123 m AMSL), located at the central part of the Indo-Gangetic Plain (IGP), experiences moderate to high levels of pollution resulting from both anthropogenic and natural emissions (Ram et al., 2010a).

To assess the probable mixing state and chemical composition of aerosols, monthly level 2 (cloud screened and quality assured) spectral AOD (0.34, 0.38, 0.44, 0.5, 0.675, and 0.87 μm) and spectral SSA (0.44, 0.675, 0.87, and 1.02 μm) measurements obtained from the AERONET (Holben et al., 2001) station at Kanpur during the period January 2007 to December 2009 are utilized. The total uncertainty associated with the measured AOD values under cloud-free conditions is estimated to be $<\pm0.01$ for wavelengths $\geq$440 nm and $<\pm0.01$ for shorter wavelengths (Smirnov et al., 2000). AOD measured at 1.02 μm is not considered for the analysis to avoid the effect of water vapor absorption.

Daytime mixed layer height (MLH) and aerosol extinction coefficient (β_{ext}) data are obtained from the NASA Micro-Pulse Lidar Network (MPLNET) Planetary Boundary Layer and Aerosol products (version 3, level 1.5), respectively (Welton et al., 2001; Lewis et al., 2013) to model the vertical distribution of mixed layer aerosols in AeroMix. The MPLNET data available over Kanpur only covers five months (May-June and October-December 2009) during the study period. Due to the lack of MPLNET data over Kanpur representing all months during the study period, seasonal averages of MLH and β_{ext} at 532 nm derived during the entire operational period of MPLNET, spanning from May 2009 to November 2015, are utilized.

The measured mass concentration of aerosols over the Kanpur is obtained from the PM_{10} aerosol samples collected during daytime (~8-10 hours) using a high-volume sampler operated at a flow rate of 1.0 ± 0.1 m^3min^{-1} on pre-combusted tissuquartz (PALLFLEX™) filters of size 20.0×25.4 cm^2 (Ram et al., 2010b). Sixty-six samples were collected during the period January 2007 to March 2008 and were analyzed for organic carbon (OC), elemental carbon (EC), water-soluble organic carbon (WSOC), and water-soluble ionic species (WSIS). No samples were collected during the monsoon season (July-September). A detailed description of the analytical procedures and the data can be found in Ram et al. (2010). The measured PM10 aerosol chemical composition is grouped into water-insoluble (IS), water-soluble (WS), black carbon (BC), sea-salt (SS), and mineral dust (MD). The mineral dust mass concentration is calculated by scaling the measured Aluminum concentration by a factor of 12.5 since the soil mass contains 8.04% of Aluminum (Srinivas et al., 2011; Taylor and McLennan, 1985). However, mineral dust mass concentration is not calculated and validated for Kanpur due to the unavailability of measured Al mass concentration. The sea-salt mass concentration is estimated by scaling the measured Na^+ mass concentration with a factor of 3.2, considering the salinity of seawater to be ~35g kg^{-1} (Millero et al., 2008). Measured EC is taken as the BC concentration. WSIS and WSOC constitute the WS mass concentration, and OC×1.6 is taken as the IS mass concentration.

Daytime relative humidity (RH) values are obtained from the automatic weather station installed at Kanpur (www.mosdac.gov.in/catalog/insitu.php) for the period November 2007 to December 2009. The availability of the collocated

aerosol chemical, optical, and vertical profile measurements make Kanpur desirable for assessing the aerosol mixing states representing an urban location.

S2.2 Bay of Bengal

BoB is located in the northeastern part of the Indian Ocean, bounded by the Indian subcontinent to the west and the Indochinese Peninsula to the east. Anthropogenic and natural emissions from these surrounding landmasses largely influence the aerosol characteristics over the BoB during winter seasons (Srinivas et al., 2011). The northwestern part of the BoB, which is most affected by the continental outflow of aerosols during the winter (Sinha et al., 2011), is selected to assess the aerosol mixing state over the marine environment.

The probable aerosol mixing state over the western and northern part of BoB (W-BoB and N-BoB) during the winter season are derived from the data obtained from the Winter-Integrated Campaign for Aerosols, gases and Radiation Budget (W-ICARB) conducted from 27th December 2008 to 30th January 2009 (Moorthy et al., 2010). W-BoB and N-BoB are demarcated following Kaskaoutis et al. (2011). The spectral AOD, MLH, RH, and aerosol chemical composition data measured from 27th December 2008 to 9th January 2009 are used in this study.

Spectral AOD (0.38, 0.44, 0.5, 0.675, and 0.87 μm) measurements were made using a handheld sunphotometer MICROTOPS-II (Solar Light Company, USA) at ~10-minute intervals. The estimated uncertainty in AOD measurements made by the MICROTOPS-II is less than ±0.03 (Morys et al., 2001; Smirnov et al., 2009). Only cloud-free data are used for the analysis, and triplet observations were made to avoid any possible operator error in sun pointing on the moving platform. For a detailed description of AOD measurements and quality controls, refer to Kaskaoutis et al. (2011).

MLH values are derived from thermodynamics variables, namely, potential temperature, wind shear, specific humidity, and bulk Richardson number. These parameters are derived from Pisharoty GPS radiosonde (make: VSSC, ISRO, India) launched daily three times at 00:30, 06:30, and 13:30 local time (LT) during the campaign. Daily mean MLH derived from 22 morning (06:30 LT) and afternoon (13:30 LT) launches were utilized in this study. A detailed description of radiosonde and methodology of the derivation of MLH are presented in Subrahamanyam et al. (2012) and thus not repeated here.

Cloud-Aerosol Lidar with Orthogonal Polarization (CALIOP) level 3, V4 cloud-free daytime extinction coefficients at 532 nm (Kim et al., 2018) were used to model the tropospheric aerosol profile over BoB. CALIOP Level 3 extinction coefficient at 532 nm is a monthly averaged globally gridded data based on quality-screened level 2 aerosol extinction profiles up to an altitude of 12 km. Cloud-free extinction coefficient profiles are quality screened following Tackett et al. (2018) and aggregated uniformly gridded onto a global 2^{o}latitudes × 5^{o}longitudes with a vertical resolution of 60 m. The incorrect LiDAR ratios (Omar et al., 2009) and aerosol type classification (Huang et al., 2013) are the two important contributors to the uncertainty in CALIOP Level 3 aerosol extinction. Despite these uncertainties, Winker et al. (2013) have shown that these Level 3 aerosol data are realistic and representative of aerosol extinction greater than about 0.001 km^{-1} and up to an altitude of 6 km. Thus, we excluded the extinction coefficient values below 0.001 km-1 in our analyses. In addition, the CALIOP Level 3 extinction coefficient has been extensively used in investigating the seasonal evolution of extinction profile

(Huang et al., 2013), global aerosol source attribution (Prijith et al., 2016), estimates of wildfire injection heights (Sofiev et al., 2013), and aerosol radiative effect (Chung et al., 2016).

Air samples containing PM10 aerosols were collected during the W-ICARB campaign over BoB onboard the ship using a high-volume sampler (Thermo Andersen, USA) 15 m above the mean sea level at a flow rate of about one m^3min^{-1} with a variation of 5%. Each sample was collected over a time period ranging from 20 to 22 h on pre-combusted tissuquartz (PALLFLEX^{TM}) filters of size $20\times25cm^2$. A total of 11 samples were collected during the cruise over W-BoB and N-BoB and were analyzed for OC, EC, WSOC, WSIS, trace metals (Cd and Pb), and crustal constituents (Al, Fe, Ca, and Mg). Detailed descriptions of the analytical procedures are given elsewhere (Srinivas et al., 2011).

RH measurements taken during the cruise using meteorological sensors onboard the ship are used to model the aerosol hygroscopic growth.

S3. Sensitivity of AOD to layer thickness

To evaluate the impact of changes in layer thickness on AOD, sensitivity analyses are conducted, keeping the vertical profiles of aerosols constant while varying MLH. Figure S3 presents the variations in mixed layer AOD at 0.5 µm in response to alterations in MLH (ΔAOD/ΔMLH). The AOD is calculated for the urban aerosol type (IS (number concentration) = 1.5 cm^{-3}, WS = 28000 cm^{-3}, and BC = 130000 cm^{-3}) at a relative humidity of 50% using AeroMix. Although the AOD changes minimally (<0.0005) for a unit meter change in MLH across the considered vertical profiles, the ΔAOD/ΔMLH is not uniform throughout the entire vertical column. Instead, it follows the distribution of aerosols within the layer. This suggests that alterations in MLH have a more pronounced effect on AOD at altitudes characterized by higher

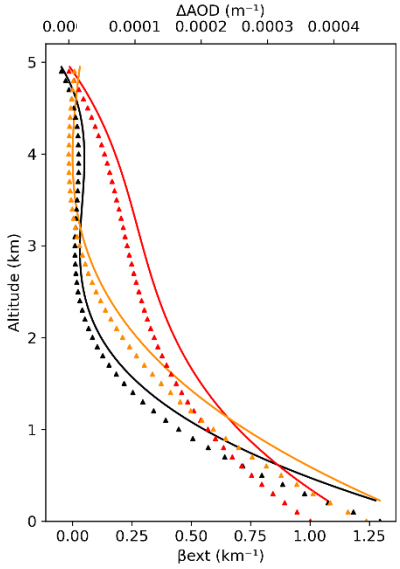

Figure S 3: Variation in mixed layer aerosol optical depth (AOD) per unit meter change in mixed layer height (MLH) across various sample vertical profiles. Calculations were performed using AeroMix for an urban aerosol type. Solid lines illustrate the sample vertical profiles, while the triangles indicate the corresponding AOD changes per unit meter change in MLH.

aerosol concentrations compared to altitudes with lower aerosol concentrations. Considering the large spatial and temporal heterogeneities in aerosol vertical profiles, a generalized quantification of the sensitivity of vertical profile assumptions on AOD lacks meaningful interpretation.

References

Chung, C. E., Chu, J. E., Lee, Y., Van Noije, T., Jeoung, H., Ha, K. J., and Marks, M.: Global fine-mode aerosol radiative effect, as constrained by comprehensive observations, Atmos. Chem. Phys., 16, 8071–8080, https://doi.org/10.5194/ACP-16-8071-2016, 2016.

Hess, M., Koepke, P., and Schult, I.: Optical Properties of Aerosols and Clouds: The Software Package OPAC, Bull. Am. Meteorol. Soc., 79, 831–844, https://doi.org/10.1175/1520-0477(1998)079<0831:OPOAAC>2.0.CO;2, 1998.

Holben, B. N., Tanré, D., Smirnov, A., Eck, T. F., Slutsker, I., Abuhassan, N., Newcomb, W. W., Schafer, J. S., Chatenet, B., Lavenu, F., Kaufman, Y. J., Vande Castle, J., Setzer, A., Markham, B., Clark, D., Frouin, R., Halthore, R., Karneli, A., O'Neill, N. T., Pietras, C., Pinker, R. T., Voss, K., and Zibordi, G.: An emerging ground-based aerosol climatology: Aerosol optical depth from AERONET, J. Geophys. Res. Atmos., 106, 12067–12097, https://doi.org/10.1029/2001JD900014, 2001.

Huang, L., Jiang, J. H., Tackett, J. L., Su, H., Fu, R., Huang, C. :, Jiang, J. H., Tackett, J. L., Su, H., and Fu, R.: Seasonal and diurnal variations of aerosol extinction profile and type distribution from CALIPSO 5-year observations, J. Geophys. Res. Atmos., 118, 4572–4596, https://doi.org/10.1002/JGRD.50407, 2013.

Kaskaoutis, D. G., Kumar Kharol, S., Sinha, P. R., Singh, R. P., Kambezidis, H. D., Rani Sharma, A., and Badarinath, K. V. S.: Extremely large anthropogenic-aerosol contribution to total aerosol load over the Bay of Bengal during winter season, Atmos. Chem. Phys., 11, 7097–7117, https://doi.org/10.5194/acp-11-7097-2011, 2011.

Kim, M. H., Omar, A. H., Tackett, J. L., Vaughan, M. A., Winker, D. M., Trepte, C. R., Hu, Y., Liu, Z., Poole, L. R., Pitts, M. C., Kar, J., and Magill, B. E.: The CALIPSO version 4 automated aerosol classification and lidar ratio selection algorithm, Atmos. Meas. Tech., 11, 6107–6135, https://doi.org/10.5194/amt-11-6107-2018, 2018.

Lewis, J. R., Welton, E. J., Molod, A. M., and Joseph, E.: Improved boundary layer depth retrievals from MPLNET, J. Geophys. Res. Atmos., 118, 9870–9879, https://doi.org/10.1002/jgrd.50570, 2013.

Millero, F. J., Feistel, R., Wright, D. G., and McDougall, T. J.: The composition of Standard Seawater and the definition of the Reference-Composition Salinity Scale, Deep Sea Res. Part I Oceanogr. Res. Pap., 55, 50–72, https://doi.org/10.1016/J.DSR.2007.10.001, 2008.

Moorthy, K. K., Beegum, S. N., Babu, S. S., Smirnov, A., John, S. R., Kumar, K. R., Narasimhulu, K., Dutt, C. B. S., and Nair, V. S.: Optical and physical characteristics of Bay of Bengal aerosols during W-ICARB: Spatial and vertical heterogeneities in the marine atmospheric boundary layer and in the vertical column, J. Geophys. Res. Atmos., 115, 24213, https://doi.org/10.1029/2010JD014094, 2010.

Morys, M., Mims, F. M., Hagerup, S., Anderson, S. E., Baker, A., Kia, J., and Walkup, T.: Design, calibration, and performance of MICROTOPS II handheld ozone monitor and Sun photometer, J. Geophys. Res. Atmos., 106, 14573–14582,

https://doi.org/10.1029/2001JD900103, 2001.

Omar, A. H., Winker, D. M., Kittaka, C., Vaughan, M. A., Liu, Z., Hu, Y., Trepte, C. R., Rogers, R. R., Ferrare, R. A., Lee, K. P., Kuehn, R. E., and Hostetler, C. A.: The CALIPSO automated aerosol classification and lidar ratio selection algorithm, J. Atmos. Ocean. Technol., 26, 1994–2014, https://doi.org/10.1175/2009JTECHA1231.1, 2009.

Prijith, S. S., Suresh Babu, S., Lakshmi, N. B., Satheesh, S. K., and Krishna Moorthy, K.: Meridional gradients in aerosol vertical distribution over Indian Mainland: Observations and model simulations, Atmos. Environ., 125, 337–345, https://doi.org/10.1016/J.ATMOSENV.2015.10.066, 2016.

Ram, K., Sarin, M. M., and Tripathi, S. N.: A 1 year record of carbonaceous aerosols from an urban site in the Indo-Gangetic Plain: Characterization, sources, and temporal variability, J. Geophys. Res. Atmos., 115, https://doi.org/10.1029/2010JD014188, 2010a.

Ram, K., Sarin, M. M., and Hegde, P.: Long-term record of aerosol optical properties and chemical composition from a high-altitude site (Manora Peak) in Central Himalaya, Atmos. Chem. Phys., 10, 11791–11803, https://doi.org/10.5194/acp-10-11791-2010, 2010b.

Sinha, P. R., Manchanda, R. K., Subbarao, J. V., Dumka, U. C., Sreenivasan, S., Suresh Babu, S., and Krishna Moorthy, K.: Spatial distribution and vertical structure of the MABL aerosols over Bay of Bengal during winter: Results from W-ICARB experiment, J. Atmos. Solar-Terrestrial Phys., 73, 430–438, https://doi.org/10.1016/j.jastp.2010.10.011, 2011.

Smirnov, A., Holben, B. N., Eck, T. F., Dubovik, O., and Slutsker, I.: Cloud-Screening and Quality Control Algorithms for the AERONET Database, Remote Sens. Environ., 73, 337–349, https://doi.org/10.1016/S0034-4257(00)00109-7, 2000.

Smirnov, A., Holben, B. N., Slutsker, I., Giles, D. M., McClain, C. R., Eck, T. F., Sakerin, S. M., Macke, A., Croot, P., Zibordi, G., Quinn, P. K., Sciare, J., Kinne, S., Harvcy, M., Smyth, T. J., Piketh, S., Zielinski, T., Proshutinsky, A., Goes, J. I., Nelson, N. B., Larouche, P., Radionov, V. F., Goloub, P., Krishna Moorthy, K., Matarrese, R., Robertson, E. J., and Jourdin, F.: Maritime Aerosol Network as a component of Aerosol Robotic Network, J. Geophys. Res. Atmos., 114, 6204, https://doi.org/10.1029/2008JD011257, 2009.

Sofiev, M., Vankevich, R., Ermakova, T., and Hakkarainen, J.: Global mapping of maximum emission heights and resulting vertical profiles of wildfire emissions, Atmos. Chem. Phys., 13, 7039–7052, https://doi.org/10.5194/ACP-13-7039-2013, 2013.

Srinivas, B., Kumar, A., Sarin, M. M., and Sudheer, a. K.: Impact of continental outflow on chemistry of atmospheric aerosols over tropical Bay of Bengal, Atmos. Chem. Phys. Discuss., 11, 20667–20711, https://doi.org/10.5194/acpd-11-20667-2011, 2011.

Subrahamanyam, D. B., Anurose, T. J., Kumar, N. V. P. K., Mohan, M., Kunhikrishnan, P. K., John, S. R., Prijith, S. S., and Dutt, C. B. S.: Spatial and temporal variabilities in vertical structure of the Marine Atmospheric Boundary Layer over Bay of Bengal during Winter Phase of Integrated Campaign for Aerosols, gases and Radiation Budget, Atmos. Res., 107, 178–185, https://doi.org/10.1016/j.atmosres.2011.12.014, 2012.

Tackett, J. L., Winker, D. M., Getzewich, B. J., Vaughan, M. A., Young, S. A., and Kar, J.: CALIPSO lidar level 3 aerosol

profile product: Version 3 algorithm design, Atmos. Meas. Tech., 11, 4129–4152, https://doi.org/10.5194/AMT-11-4129-2018, 2018.

Taylor, S. R. and McLennan, S. M.: The continental crust, its composition and evolution : an examination of the geochemical record preserved in sedimentary rocks, Blackwell Scientific Publications, Oxford ; Melbourne, 1985.

Welton, E. J., Campbell, J. R., Spinhirne, J. D., and III, V. S. S.: Global monitoring of clouds and aerosols using a network of micropulse lidar systems, in: Lidar Remote Sensing for Industry and Environment Monitoring, 151–158, https://doi.org/10.1117/12.417040, 2001.

Winker, D. M., Tackett, J. L., Getzewich, B. J., Liu, Z., Vaughan, M. A., and Rogers, R. R.: The global 3-D distribution of tropospheric aerosols as characterized by CALIOP, Atmos. Chem. Phys., 13, 3345–3361, https://doi.org/10.5194/ACP-13-3345-2013, 2013.